Published in final edited form as:
Biochim Biophys Acta. 2009 August ; 1791(8): 806–815. doi:10.1016/j.bbalip.2009.05.006.

Mitochondrial long chain fatty acid β-oxidation in man and mouse

Malika Chegary[a,b], **Heleen te Brinke**[a], **Jos P.N. Ruiter**[a], **Frits A. Wijburg**[b], **Maria S.K. Stoll**[c], **Paul E. Minkler**[c], **Michel van Weeghel**[a], **Horst Schulz**[e], **Charles L. Hoppel**[c,d], **Ronald J.A. Wanders**[a,b], and **Sander M. Houten**[a,b]

[a]Department of Clinical Chemistry, Laboratory Genetic Metabolic Diseases, Emma Children's Hospital, Academic Medical Center, University of Amsterdam, Meibergdreef 9, 1105 AZ Amsterdam, The Netherlands [b]Department of Pediatrics, Emma Children's Hospital, Academic Medical Center, University of Amsterdam, Meibergdreef 9, 1105 AZ Amsterdam, The Netherlands [c]Department of Pharmacology, Case Western Reserve University School of Medicine, Cleveland OH 44106 [d]Department of Medicine, Case Western Reserve University School of Medicine, Cleveland OH 44106 [e] Department of Chemistry, City College and Graduate Center of the City University of New York, New York, USA

Summary

Several mouse models for mitochondrial fatty acid β-oxidation (FAO) defects have been developed. So far, these models have contributed little to our current understanding of the pathophysiology. The objective of this study was to explore differences between murine and human FAO. Using a combination of analytical, biochemical and molecular methods, we compared fibroblasts of long chain acyl-CoA dehydrogenase knockout ($LCAD^{-/-}$), very long chain acyl-CoA dehydrogenase knockout ($VLCAD^{-/-}$) and wild type mice with fibroblasts of VLCAD-deficient patients and human controls. We show that in mice, LCAD and VLCAD have overlapping and distinct roles in FAO. The absence of VLCAD is apparently fully compensated, whereas LCAD deficiency is not. LCAD plays an essential role in the oxidation of unsaturated fatty acids such as oleic acid, but seems redundant in the oxidation of saturated fatty acids. In strong contrast, LCAD is neither detectable at the mRNA level nor at the protein level in men, making VLCAD indispensable in FAO. Our findings open new avenues to employ the existing mouse models to study the pathophysiology of human FAO defects.

Keywords

cellular metabolism; inborn errors of metabolism; fatty acid oxidation; mouse models; long chain acyl-CoA dehydrogenase; very long chain acyl-CoA dehydrogenase

Address correspondence to Sander Houten, PhD: Laboratory Genetic Metabolic Diseases (F0-222), Academic Medical Center, University of Amsterdam, Meibergdreef 9, 1105 AZ Amsterdam, The Netherlands. Phone: +31 20 566 5958, Fax: +31 20 696 2596, E-mail: s.m.houten@amc.uva.nl.

Introduction

Mitochondrial fatty acid β-oxidation (FAO) is essential for energy production, in particular, during periods of fasting and other metabolic stress conditions. Fatty acids are oxidized in a cycle of four subsequent reactions: dehydrogenation, hydration, a second dehydrogenation and thiolytic cleavage. After each cycle, an acyl-CoA is shortened by two carbon atoms and an acetyl-CoA is generated. The first reaction of the β-oxidation spiral is performed by acyl-CoA dehydrogenases (ACADs) that catalyze the formation of a trans- α, β double bond. Different ACADs are known, each with a specificity determined by the properties of the acyl group. These include very long chain acyl-CoA dehydrogenase (VLCAD), long chain acyl-CoA dehydrogenase (LCAD), acyl-CoA dehydrogenase 9 (ACAD9), medium chain acyl-CoA dehydrogenase (MCAD) and short chain acyl-CoA dehydrogenase (SCAD). FAO deficiency caused by ACAD defects are among the most common inborn errors of metabolism. Patients typically accumulate intermediate metabolites (acylcarnitines) with profiles that reflect the substrate use of the deficient enzyme in tissues or cells [1,2].

The main pathological consequences associated with FAO deficiency are hypoketotic hypoglycaemia, metabolic acidosis, hyperammonemia and fatty liver, which can all be prevented by the avoidance of fasting. Cardiac abnormalities and myopathy are only described in patients with deficiencies affecting long chain FAO, like carnitine palmitoyltransferase 2 (CPT2) deficiency, carnitine-acylcarnitine translocase deficiency, VLCAD deficiency (VLCADD) and defects in mitochondrial trifunctional protein (MTP) including long chain 3-hydroxyacyl-CoA dehydrogenase deficiency [3–6]. Until now, no patients with LCAD deficiency have been identified. Previously reported patients with LCAD deficiency were later shown to be VLCAD deficient [7].

There is still a lack of therapeutic options to effectively prevent or causally treat the cardiac signs and symptoms related to long chain FAO defects. Roe et al showed improvement of cardiomyopathy and rhabdomyolysis in VLCAD and CPT2 patients treated with an anaplerotic odd-chain triglyceride [8,9]. However, this treatment needs to be confirmed in a larger cohort of patients.

Better understanding of the pathophysiological processes leading to cardiac disease in long chain FAO defects is needed in order to design new therapeutics. To this end, several mouse models have been developed. Mouse models are usually selected based on similarities in phenotype and genetic defect. The characterized mouse models include deficiencies of VLCAD, LCAD, MTP, CPT1a and CPT1b. The phenotype of these mouse models differ in severity. The VLCAD knockout ($VLCAD^{-/-}$) mouse has a surprisingly mild phenotype consisting of mild hepatic steatosis and mild fatty change in the heart in response to fasting or cold challenge [10–12]. Exil et al further characterized the $VLCAD^{-/-}$ hearts and demonstrated microvesicular lipid accumulation, marked mitochondrial proliferation, and facilitated induction of polymorphic ventricular tachycardia, without preceding stress [11,13]. The LCAD knockout ($LCAD^{-/-}$) mouse has a more severe phenotype, more closely resembling human VLCADD [10,14]. Characteristics include fasting-induced hypoketotic hypoglycemia and marked fatty changes in liver and heart. The $MTP^{-/-}$, $CPT1a^{-/-}$ as well as $CPT1b^{-/-}$ mice have very severe phenotypes [15–17]. The $MTP^{-/-}$ mouse model is lethal in the neonatal period [15] and both $CPT1a^{-/-}$ and $CTP1b^{-/-}$ mice are embryonic lethal [16,17], which complicates studies. Further characterization of the available mouse models may help to elucidate the pathogenesis of FAO disorders. We therefore studied differences in mitochondrial FAO between man and mouse by comparing human VLCADD fibroblasts and fibroblasts of two mouse models, the $VLCAD^{-/-}$ and $LCAD^{-/-}$ mouse.

Material and methods

Materials

Myristic acid (C14:0), myristoleic acid (C14:1(n-5) or *cis*-tetradec-9-enoic acid), palmitic acid (C16:0), palmitoleic acid (C16:1(n-7)), stearic acid (C18:0), oleic acid (C18:1(n-9)) and linoleic acid (C18:2(n-6)) were purchased from Sigma. Physeteric acid (C14:1(n-9) or *cis*-tetradec-5-enoic acid) was synthesized as described [18]. [9,10-^{3}H(N)] oleic acid was purchased from PerkinElmer and bovine serum albumin (BSA, fatty acid free) from Sigma. The internal standards d3-C3-, d3-C8- and d3-C16-acylcarnitine were obtained from Dr. Herman J. ten Brink (VU Medical Hospital, The Netherlands). pYes2.0-CPT1a was provided by dr. Carina Prip-Buus. All other reagents were of analytical grade.

Animals

LCAD$^{+/-}$ (B6.129S6-*Acadl*^{tm1UAB}/Mmmh) [14] on a pure C57BL/6 background were obtained from mutant mouse regional resource centers. Male LCAD$^{-/-}$ and LCAD$^{+/+}$ mice were generated and liver fatty acid profile was analyzed at 6 months of age (n = 4–6 per group). For the fed condition, mice were placed in a clean cage at 8 am and sacrificed 4 to 6 hours later. For the fasted condition, mice were placed in a clean cage at 4 pm and fasted overnight (16 to 20 hours).

Cell culture

Human skin fibroblasts were from controls and a VLCADD patient, homozygous for a c.AGTT798del mutation. Fibroblasts from ears of wild-type (WT) and VLCAD$^{-/-}$ were a gift from Dr. Wood, University of Alabama. These mice were on a mixed background [10]. Fibroblast cell lines from WT and LCAD$^{-/-}$ mice on a pure C57BL/6 background were established from the tail tip. All fibroblasts cell lines were cultured in Ham's F10 medium (Gibco) with glutamine, 10% fetal bovine serum (Gibco), 1% mixture of penicillin, streptomycin, fungizone (Gibco) and incubated in a humidified CO_2 incubator (5% CO_2, 95% air) at 37°C.

Overexpression of human LCAD

293 (human embryo kidney) cells were transfected with pcDNA3-human LCAD or empty pcDNA3 using lipofectamine 2000 (Invitrogen), according to the instructions of the manufacturer.

Synthesis of acylcarnitines

The C14:1(n-9) and C14:1(n-5) acyl-CoA esters were synthesized as described [19]. These CoA esters were converted into the corresponding carnitine esters using recombinant rat CPT1a expressed in *Saccharomyces cerevisiae* as described [20,21].

Acylcarnitine analysis

Fibroblasts were cultured in 12 well plates at 37°C, 5% CO_2 in MEM medium (Gibco) containing 1% mixture of penicillin, streptomycin, fungizone and 0.4mM L-carnitine, 0.4% (w/v) BSA and 100μM of saturated or unsaturated fatty acids as indicated in the figure. After 72 hours the incubation was stopped by removing the medium from the cells. The medium was diluted 1:1 with water containing internal standards (50pmol d3-C3-, 20pmol d3-C8-, and 20pmol d3-C16-carnitine). Subsequently, acetonitrile was added to deproteinise the medium. Samples were centrifuged and the supernatant collected and dried at 45°C under N_2, followed by butylation for 15 minutes at 60°C using 1-butanol/acetylchloride (4:1), drying at 45°C under N_2, and dissolving the samples in acetonitrile. Quantitative determination of the formed acylcarnitines in the medium was performed using tandem mass spectrometry [22]. The cells

were washed twice with PBS and dissolved with 0.1% (v/v) Triton X-100 in PBS. Protein concentration was determined using BCA reagent. The same assay was performed by incubating fibroblasts with 100 μM [U-^{13}C]-oleic acid, in the presence of 0.4% or 0.1% (w/v) BSA. The formed [U-^{13}C]-acylcarnitines were quantified by tandem mass spectrometry as described above. HPLC MS-MS analysis of acylcarnitine pentafluorophenacyl esters was performed as described by Minkler et al [23,24].

Fatty acid oxidation

Oleic acid oxidation was measured by quantifying the production of $^{3}H_2O$ from [9,10-^{3}H(N)] oleic acid as described previously by Manning et al [25]. Briefly, the fibroblasts were trypsinized, plated in 48-well plates and allowed to adhere overnight. Assays were performed in quadruplicate. The β-oxidation assay was carried out for 2 hr at 37°C cells in Krebs-Henselheit buffer containing 0.1% or 0.4% (w/v) BSA, 100μM oleic acid and a tracer of [9,10-^{3}H] oleic acid. The reaction was stopped by applying the medium to an ion-exchange column containing Dowex-OH^- (1×8-200; Sigma-Aldrich). The columns were washed twice with water and the radioactivity of the eluate was determined using liquid scintillation counting. Protein concentration was determined using BCA reagent (Sigma). Oleic acid oxidation rates were expressed as nmol of fatty acid oxidized per hour per milligram of cell protein (nmol/h.mg). The oleic acid oxidation in soleus muscle was measured as described above. The incubation time was 30 minutes. Oleic acid oxidation rates were expressed as pmol of fatty acid oxidized per minute corrected for the wet weight of the tissue (pmol/min.mg).

Quantitative real-time RT-PCR analysis

Total RNA was isolated from human and mouse fibroblasts using Trizol (Invitrogen) extraction, after which cDNA was prepared using the Superscript II Reverse Transcriptase kit (Invitrogen). Quantitative real-time PCR analysis of MCAD, LCAD, VLCAD, ACAD9 and cyclophilin-B of both human and mouse was performed in this cDNA using the LC480 Sybr Green I Master mix (Roche). Primer sequences are available upon request. To confirm the amplification of a single product both melting curve analysis and sequence analysis was carried out. All samples were analyzed in duplicate. Data were analyzed using linear regression analysis as described by Ramakers et al [26]. To compare the MCAD, LCAD, VLCAD and ACAD9 expression between different samples, values were normalized against the values for the housekeeping gene cyclophilin-B.

Gene expression profile of VLCAD and LCAD

The gene expression profile of VLCAD and LCAD as suggested by the analysis of expressed sequence tags (EST) counts was performed by expression profile analysis at the UniGene database of NCBI.

Acyl-CoA dehydrogenase enzyme measurements

Acyl-CoA dehydrogenase activity was determined in homogenates of human and mouse fibroblasts by using ferricenium hexafluorophosphate as electron acceptor followed by HPLC to separate the different acyl-CoA species [27]. C16:0-CoA, C18:1-CoA and 2,6-dimethylheptanoyl-CoA (DMH-CoA) were used as substrates.

Immunoblot

The rabbit anti rat LCAD antibodies were a gift from Dr. T. Hashimoto, Shinshu University, Matsumoto, Japan [28].

Fatty acid analysis

Liver tissue was homogenized using a dispersion tool (Ika T10 basic). After sonication (twice at 8W output, 40J, on ice), protein concentration was measured and all samples were diluted to 2mg/mL. Fatty acids from a 100μg sample were directly transesterified and analyzed by gas chromatography with flame ionization detection [29].

Results

Acylcarnitine accumulation of the LCAD$^{-/-}$ mouse resembles human VLCADD

Routine biochemical diagnosis of FAO disorders is carried out by detection of abnormal concentrations of acylcarnitines in body fluids using tandem mass spectrometry. The diagnosis of VLCADD is predominantly based on elevated plasma levels of C14:1 acylcarnitine and other long chain acylcarnitines like C18:1 and C16:0 acylcarnitine. Similar analyses performed in VLCAD$^{-/-}$ and LCAD$^{-/-}$ mice, showed a small increase of plasma C16-C18 acylcarnitines in the VLCAD$^{-/-}$ after exercise and fasting in the cold, and a prominent elevation of C14:1 acylcarnitine in the LCAD$^{-/-}$ mouse [10,12,14]. In order to determine to what extent LCAD$^{-/-}$ and VLCAD$^{-/-}$ mice resemble human VLCADD, we incubated the respective fibroblasts with different saturated and unsaturated fatty acids. The formation of acylcarnitines was measured in the culture medium.

Human VLCADD fibroblasts accumulate acylcarnitines after incubation with saturated and unsaturated fatty acids. Interestingly, incubation with palmitic acid leads to accumulation of C16 and C14 acylcarnitine (Figure 1A), whereas upon incubation with oleic acid C18:1, there is accumulation of C16:1 and C14:1 acylcarnitine, indicative of low residual FAO (Figure 1B). The acylcarnitine profile in culture medium of LCAD$^{-/-}$ fibroblasts resembles human VLCADD more than the profile observed in the culture medium of VLCAD$^{-/-}$ fibroblasts. Especially after incubation with unsaturated fatty acids there is a marked acylcarnitine accumulation. Treatment with oleic acid leads to accumulation of C14:1 acylcarnitine (Figure 1B), whereas treatment with linoleic acid causes C14:2 acylcarnitine accumulation (Figure 1C). Incubation with palmitic acid leads to low C12 acylcarnitine accumulation (Figure 1A). In VLCAD$^{-/-}$ fibroblasts there is no significant acylcarnitine accumulation with any of the substrates.

To investigate whether the accumulating acylcarnitines in the culture medium are similar to the plasma acylcarnitines in VLCADD patients and LCAD$^{-/-}$ mice, we derivatized the acylcarnitines with pentafluorophenacyl trifluoromethanesulfonate and used HPLC MS/MS. Using this method, we are able to separate acylcarnitine pentafluorophenacyl ester constitutional isomers [23,24]. In both plasma of a VLCADD patient and the LCAD$^{-/-}$ mouse, C14:1 acylcarnitine was elevated (Figure 2A). Two isomeric forms of C14:1 acylcarnitine were observed, one abundant C14:1 acylcarnitine pentafluorophenacyl ester and a minor isoform visible as a small shoulder on the major C14:1 acylcarnitine pentafluorophenacyl ester peak (Figure 2B). The most abundant of this C14:1 acylcarnitine isomer was also observed in medium of LCAD$^{-/-}$ mouse fibroblasts incubated with oleic acid (Figure 2A, B). Moreover, upon linoleic acid treatment of these fibroblasts, a C14:2 acylcarnitine was formed that was also detected in plasma of both the human VLCADD patient and the LCAD$^{-/-}$ mouse (Figure 2A). These results indicate that deficient oleic- and linoleic acid oxidation is responsible for the increased C14:1 and C14:2 acylcarnitine detected in the plasma of LCAD$^{-/-}$ mice. Moreover, it suggests that C14:1(n-9) acylcarnitine formed after 2 cycles of oleic acid oxidation, is the most abundant C14:1 acylcarnitine in plasma of VLCADD patients and the LCAD$^{-/-}$ mouse. A similar conclusion for VLCADD was made based on the analysis of free fatty acid and total fatty acid profiles in plasma [30].

To obtain additional evidence for the identity of these acylcarnitines, we prepared and analyzed C14:1(n-5), C14:1(n-9) and t-C14:1(n-12) (*trans*-tetradec-2-enoic) acylcarnitine pentafluorophenacyl esters. Interestingly, C14:1(n-9) acylcarnitine pentafluorophenacyl ester has a specific fragment ion (m/z 311) that is not observed for C14:1(n-5) and t-C14:1(n-12) acylcarnitine pentafluorophenacyl esters (Figure 2C, D). The major C14:1 acylcarnitine pentafluorophenacyl ester in VLCADD and LCAD$^{-/-}$ plasma is C14:1(n-9) acylcarnitine pentafluorophenacyl ester based on the MS/MS chromatogram for the m/z 311 ion and the retention time (Figure 2B).

Differences in C14:1 oxidation between human and mouse

Next, we studied the oxidation of C14:1 in more detail. Interestingly, incubation with C14:1 (n-5) did not lead to an increased C14:1 acylcarnitine level in LCAD$^{-/-}$ fibroblasts, whereas in VLCADD fibroblasts there was C14:1 acylcarnitine accumulation (Figure 3). This suggests that mouse LCAD reacts differently on the C14:1(n-9)-CoA. Therefore, we reasoned that the position of the double bond in C14:1-CoA is essential for mouse LCAD activity. To further investigate this, we incubated human VLCADD fibroblasts and mouse VLCAD$^{-/-}$ and LCAD$^{-/-}$ fibroblasts also with C14:1(n-9). Incubation with C14:1(n-9) caused accumulation of C14:1 acylcarnitine in human VLCADD as well as LCAD$^{-/-}$ fibroblasts, whereas C14:1 (n-5) only caused accumulation of C14:1 acylcarnitine in human VLCADD fibroblasts (Figure 3). In VLCAD$^{-/-}$ fibroblasts none of the substrates resulted in elevated levels of acylcarnitine (Figure 3). In conclusion, in human fibroblasts the length of the acyl-CoA determines whether human VLCAD is active, whereas in mouse fibroblasts the position of the double bond determines the reactivity of mouse LCAD.

Mild FAO deficiency in the LCAD$^{-/-}$ fibroblasts

Since oleic acid treatment revealed interesting differences in acylcarnitine accumulation, we determined the rate of oleic acid oxidation in all fibroblast cell lines. Oleic acid oxidation was severely impaired in human VLCADD fibroblasts, but not in the VLCAD$^{-/-}$ and LCAD$^{-/-}$ fibroblasts (Figure 4A). Although this confirms to some degree the milder acylcarnitine accumulation in these mouse cell lines, the completely normal oleic acid oxidation rate in the LCAD$^{-/-}$ fibroblasts was unexpected based on our observations described above. We reasoned that by increasing the workload on the FAO pathway, oleic acid oxidation impairment might become evident in LCAD$^{-/-}$ fibroblasts as well. Therefore, we decreased the BSA concentration from 0.4% to 0.1% while keeping the oleic acid concentration constant. Interestingly, the higher free fatty acid levels caused an increase in the rate of oleic acid oxidation in wild-type and VLCAD$^{-/-}$ mouse fibroblasts, but not in the LCAD$^{-/-}$ fibroblasts (Figure 4B). Thus, increasing FAO flux by lowering the BSA concentration uncovered the defect in oleic acid oxidation in LCAD$^{-/-}$ fibroblasts.

To obtain additional proof for the deficiency of oleic acid oxidation in LCAD$^{-/-}$ fibroblasts, we quantified the production of C2-acylcarnitine from [U-^{13}C] oleic acid. Lowering the BSA concentration from 0.4% to 0.1% increased acetylcarnitine production in wild type mouse fibroblasts, indicating an increase in oleic acid oxidation. Interestingly, LCAD$^{-/-}$ fibroblasts did not raise acetylcarnitine production suggesting that the FAO rate could not increase further (Figure 4C). This perfectly mirrors the results obtained with the oleic acid oxidation assay.

In order to verify whether a similar deficiency can also be observed in LCAD$^{-/-}$ mouse tissue, we measured the oleic acid oxidation rate in isolated soleus muscle. As in fibroblasts, soleus muscle of LCAD$^{-/-}$ mice had deficient oleic acid oxidation (Figure 4D).

Differences in the expression of ACAD enzymes

We hypothesized that substrate overlap between LCAD and VLCAD or other acyl-CoA dehydrogenases in mice could explain the biochemical differences and the relatively mild phenotype in the LCAD$^{-/-}$ and VLCAD$^{-/-}$ mouse models when compared with human VLCADD. To test if there are differences in the expression levels of the different acyl-CoA dehydrogenases between human and mouse fibroblasts, we used Q-RT-PCR (Figure 5A). In human VLCADD, neither ACAD9 nor MCAD expression was changed. LCAD expression was undetectable in both control and VLCADD fibroblasts. In this particular VLCADD patient, VLCAD expression was lower, most probably because the mutation leads to an unstable mRNA. In both VLCAD$^{-/-}$ and LCAD$^{-/-}$ fibroblasts, there were no marked differences in expression levels of other ACADs. In LCAD$^{-/-}$ fibroblasts, ACAD9 expression was slightly elevated. The VLCAD mRNA was unstable in the VLCAD$^{-/-}$ fibroblasts, whereas the LCAD mRNA was stable in the LCAD$^{-/-}$ fibroblasts. In contrast to human fibroblasts, LCAD expression is readily detectable in mouse fibroblasts. Aoyama et al also suggested that LCAD is expressed at low levels in human cells and tissues. This could provide an attractive explanation for the differences in the long chain FAO between human and mice [31,32].

We looked for additional evidence for this difference in LCAD expression using the gene expression profile analysis of the UniGene database (Figure 5B). This analysis shows that VLCAD ESTs are abundantly present in human and mouse tissues. For LCAD the situation is entirely different. Numerous LCAD ESTs are present in mouse tissues, whereas only few ESTs are found for human tissues. These data further strengthen the hypothesis that differences in FAO between human and mouse are primarily caused by differences in LCAD expression.

Besides LCAD expression analysis we also performed immunoblot analysis by using an LCAD antibody on lysates of these cell lines (Figure 5C). LCAD protein was detectable in mouse fibroblasts, whereas it was not in human fibroblasts, which is in line with the expression data. Furthermore, LCAD was not detectable in the LCAD$^{-/-}$ fibroblasts, confirming the original data showing that in this mouse model, the LCAD protein is unstable [14]. To prove that the LCAD antibody recognizes human LCAD, we overexpressed human LCAD in 293 cells using transient transfection. In 293 cells transfected with an empty plasmid, LCAD protein is undetectable. After transfection of the human cDNA encoding LCAD, expression is detected in abundance (Figure 5D). In addition, we included a human liver and a human heart homogenate and compared LCAD protein levels with mouse liver. LCAD protein levels were very low in human liver and heart, suggesting that also in vivo in humans LCAD is expressed at low level, confirming the fibroblast data (Figure 5D).

To determine the degree of functional overlap in long chain acyl-CoA dehydrogenases, we performed enzyme analysis using C16:0-CoA, C18:1-CoA and DMH-CoA as substrates. In human VLCADD fibroblast lysates C16:0-CoA as well as C18:1-CoA dehydrogenation was completely deficient, indicating there are no other ACADs that significantly contribute to the oxidation of these substrates (Figure 5E). In contrast to the human situation, no reduction in C16:0-CoA and C18:1-CoA dehydrogenation was observed in the VLCAD$^{-/-}$ fibroblast extracts. Taken into account that VLCAD$^{-/-}$ fibroblasts also showed minor changes in acylcarnitine profile and no impaired oleic acid oxidation, this suggests that a deficiency of VLCAD is compensated by other ACADs such as LCAD. In the LCAD$^{-/-}$ fibroblast homogenates, the dehydrogenation of C16:0-CoA as well as C18:1-CoA was reduced, but not absent (Figure 5D). This suggests that the deficiency of LCAD is partially compensated by other ACADs such as VLCAD.

As expected, DMH-CoA dehydrogenation was virtually undetectable in the LCAD$^{-/-}$ fibroblasts, since DMH-CoA is a specific substrate for LCAD as previously shown by us

[33]. In human fibroblasts, we observed very low DMH-CoA activities, which can be explained by the fact that LCAD is not expressed in human fibroblasts (Figure 5D).

Fatty acid profile in LCAD$^{-/-}$ mice

To obtain in vivo evidence for the role of LCAD in the oxidation of unsaturated fatty acids, we determined the hepatic fatty acid profile in LCAD$^{-/-}$ mice and wild type littermates in the fed and fasted state. In the fed state, there are no significant differences in total fatty acid content and the relative contributions of the different saturated (SFA), monounsaturated (MUFA) and polyunsaturated fatty acids (PUFA) (Figure 6A, B). After an overnight fast, LCAD$^{-/-}$ mice have a fatty liver as evidenced by an increased liver weight (not shown) and higher total fatty acid content (Figure 6A). Under this condition, the relative contribution of SFA was lower in LCAD$^{-/-}$ livers, whereas the MUFA content was higher. The contribution of PUFA was not changed (Figure 6B). Analysis of the relative contribution of individual fatty acids showed that this difference was primarily caused by a decrease in C16:0 and an increase in C18:1(n-9) and C16:1(n-7) (Figure 6C). These results are consistent with a role of LCAD in the oxidation of unsaturated fatty acids.

Discussion

To obtain insight in the pathogenesis of FAO disorders, several mouse models of these inborn errors have been developed and characterized. The objective of this study was to explore differences in the FAO pathway of man and mouse and to study two mouse models for human VLCADD. Therefore we compared mitochondrial FAO of LCAD$^{-/-}$ and VLCAD$^{-/-}$ mouse fibroblasts with fibroblasts of human VLCADD patients, using a combination of analytical, biochemical and molecular methods. Previous studies showed that the phenotype of the LCAD$^{-/-}$ mouse is more severe compared to the VLCAD$^{-/-}$ mouse [10]. In addition, the LCAD$^{-/-}$ mouse displays some of the clinical and metabolic features of patients with VLCADD [14]. In this study we show that the acylcarnitine profile as observed in medium of LCAD$^{-/-}$ fibroblasts compares relatively well with the profile produced in human VLCADD fibroblasts after incubation with unsaturated fatty acids. Nevertheless, the LCAD$^{-/-}$ mouse also differs from human VLCADD fibroblasts in certain aspects. We observed differences in the degradation of C14:1-CoA. In humans, the length of these CoA-esters determines that it will be handled by VLCAD. In mouse the position of the double bond determines that it is handled preferentially by LCAD. Supportive data have been reported by Le and Yu et al, who demonstrated that in vitro C14:1(n-9)-CoA is effectively dehydrogenated by purified LCAD, whereas it was a poor substrate of VLCAD [34,35]. Interestingly, in human fibroblasts, VLCAD is largely responsible for the dehydrogenation of C14:1(n-9)-CoA [36]. This is illustrated by the accumulation of C14:1 acylcarnitine after incubation with oleic acid (Figure 1).

Furthermore, we observed major differences in the severity of the mitochondrial FAO deficiency in fibroblasts of both mouse models and the human VLCADD patient. In human VLCADD, oleic acid oxidation was severely deficient. In contrast, oleic acid oxidation and, in addition, palmitic acid and myristic acid oxidation (data not shown) were not impaired in the VLCAD$^{-/-}$ fibroblasts consistent with the mild phenotype of the mouse model. Interestingly, despite evident C14:1 acylcarnitine accumulation, oleic acid oxidation in LCAD$^{-/-}$ fibroblasts was normal. Importantly, when the free fatty acid level was increased by decreasing the concentration of BSA in the medium, a (partial) deficiency of oleic acid oxidation did become apparent. Control fibroblasts were able to increase their FAO rate, whereas LCAD$^{-/-}$ fibroblasts were not. This was further substantiated by a decreased acetylcarnitine production from oleic acid. These results strongly suggest that VLCAD$^{-/-}$ and

LCAD$^{-/-}$ mice have a relatively mild phenotype due to the functional overlap of ACADs that is absent in humans.

We provide evidence that the differences in FAO between man and mouse are primarily caused by a difference in LCAD expression levels. Analysis of the gene expression profile using the EST database showed that in mice both LCAD and VLCAD are expressed, whereas in most of the human tissues LCAD ESTs are absent or scarce. We now show that in human fibroblasts, LCAD is not detectable at the mRNA level nor at the protein level. In human heart and liver, LCAD protein level was also very low. In agreement with our results, extremely low LCAD mRNA expression levels were measured in different human tissues by He et al [37]. Therefore, we believe that LCAD does not play an essential role in FAO in most human tissues. In contrast to the situation in man, substrate overlap between VLCAD and LCAD could explain the mild phenotype in the LCAD$^{-/-}$ and VLCAD$^{-/-}$ mice.

We determined the degree of substrate overlap between different ACADs by enzyme assays using different long chain acyl-CoAs. C16:0-CoA and C18:1-CoA dehydrogenation was severely deficient in VLCADD fibroblasts. The long chain-CoA dehydrogenation was less reduced in the LCAD$^{-/-}$ fibroblasts and normal in the VLCAD$^{-/-}$ fibroblasts. Similar results have been reported in liver, heart and skeletal muscle extracts of LCAD$^{-/-}$ and VLCAD$^{-/-}$ mice [10]. In addition, Kurtz et al measured a 28% reduction in the ability to dehydrogenate C16:0-CoA in extracts from LCAD$^{-/-}$ fibroblasts [14]. By using a VLCAD antibody that blocks VLCAD activity they further showed that the residual activity in the LCAD$^{-/-}$ fibroblasts towards C16:0-CoA was the result of VLCAD activity. This proves that in mice there is substrate overlap between LCAD and VLCAD, which is absent in humans. This is further supported by the fact that breeding of the VLCAD$^{-/-}$ mice with LCAD$^{-/-}$ mice does not produce live double knockout mice [10].

Finally, we have provided in vivo evidence for a role of LCAD in the oxidation of unsaturated fatty acids. First, oleic acid oxidation was deficient in LCAD$^{-/-}$ soleus muscle. Second, fasting changed the hepatic fatty acid profile of LCAD$^{-/-}$ mice, SFA decreased and MUFA increased, strongly suggesting preferential oxidation of SFA.

The differences in LCAD expression between human and mouse could be caused by changes in the LCAD promoter region. As coding regions of proteins, promoters also contain well conserved DNA sequences. Database searches revealed that the mouse LCAD promoter has no significant homology with the human LCAD promoter [38,39]. The mouse LCAD promoter is homologous to the rat promoter, whereas the human promoter is homologous to the chimpanzee promoter (data not shown). This suggests that the LCAD promoter region dramatically changed after divergence of the rodent and primate lineage. It is, however, at this moment not clear if this is related to the loss high LCAD expression levels. For this LCAD expression levels have to be analyzed in primates such as the chimpanzee.

Several in vitro studies have suggested a role for ACAD9 in long chain FAO based on experiments with purified recombinant ACAD9. This enzyme was active with many long chain (unsaturated) acyl-CoAs [37,40]. Immunoinactivation experiments combined with immunohistochemical and immunofluoresent staining suggest an important role for ACAD9 in brain [37]. Although ACAD9 is well expressed in human and mouse fibroblasts, we found no evidence for functional overlap between VLCAD and LCAD. For functional studies on ACAD9, the generation of a knockout mouse seems instrumental.

It is remarkable that despite the absence of detectable long chain acyl-CoA dehydrogenase activity in VLCADD patients, long-chain acyl-CoAs do undergo a few cycles of FAO. This has been shown before and is for example illustrated by the accumulation of C16:1 and C14:1 acylcarnitines after incubation with oleic acid as well as by the residual activity in the oleic

acid oxidation (Figure 1 and Figure 4a) [36]. Since it is C14:1(n-9) that accumulates in human VLCADD, it is tempting to speculate that this residual activity is not LCAD activity, but MCAD or ACAD9. Selective inhibition of these enzymes, using inhibitors or RNAi is expected to resolve this issue.

In conclusion, our results show that there is a significant overlap in function of the VLCAD and LCAD enzyme in the mouse, which is in contrast to the remarkable absence of significant LCAD function in man. Our findings offer an explanation for the different phenotypic presentation of these FAO defects in man and mouse.

Acknowledgements

The authors thank Sacha Ferdinandusse and Simone Denis for helpful discussions. This work was supported by the Netherlands Organisation for Scientific Research (VIDI-grant No. 016.086.336 to SMH) and the NIH (DK066107 to CLH).

References

1. Rinaldo P, Matern D, Bennett MJ. Fatty acid oxidation disorders. Annu. Rev. Physiol 2002;64:477–502. [PubMed: 11826276]
2. Wanders RJ, Vreken P, den Boer ME, Wijburg FA, van Gennip AH, IJlst L. Disorders of mitochondrial fatty acyl-CoA beta-oxidation. J. Inherit. Metab Dis 1999;22:442–487. [PubMed: 10407780]
3. den Boer ME, Wanders RJ, Morris AA, IJlst L, Heymans HS, Wijburg FA. Long-chain 3-hydroxyacyl-CoA dehydrogenase deficiency: clinical presentation and follow-up of 50 patients. Pediatrics 2002;109:99–104. [PubMed: 11773547]
4. Mathur A, Sims HF, Gopalakrishnan D, Gibson B, Rinaldo P, Vockley J, Hug G, Strauss AW. Molecular heterogeneity in very-long-chain acyl-CoA dehydrogenase deficiency causing pediatric cardiomyopathy and sudden death. Circulation 1999;99:1337–1343. [PubMed: 10077518]
5. Saudubray JM, Martin D, de Lonlay P, Touati G, Poggi-Travert F, Bonnet D, Jouvet P, Boutron M, Slama A, Vianey-Saban C, Bonnefont JP, Rabier D, Kamoun P, Brivet M. Recognition and management of fatty acid oxidation defects: a series of 107 patients. J. Inherit. Metab Dis 1999;22:488–502. [PubMed: 10407781]
6. Vianey-Saban C, Divry P, Brivet M, Nada M, Zabot MT, Mathieu M, Roe C. Mitochondrial very-long-chain acyl-coenzyme A dehydrogenase deficiency: clinical characteristics and diagnostic considerations in 30 patients. Clin. Chim. Acta 1998;269:43–62. [PubMed: 9498103]
7. Yamaguchi S, Indo Y, Coates PM, Hashimoto T, Tanaka K. Identification of very-long-chain acyl-CoA dehydrogenase deficiency in three patients previously diagnosed with long-chain acyl-CoA dehydrogenase deficiency. Pediatr 1993;34:111–113.
8. Roe CR, Sweetman L, Roe DS, David F, Brunengraber H. Treatment of cardiomyopathy and rhabdomyolysis in long-chain fat oxidation disorders using an anaplerotic odd-chain triglyceride. J. Clin. Invest 2002;110:259–269. [PubMed: 12122118]
9. Roe CR, Yang BZ, Brunengraber H, Roe DS, Wallace M, Garritson BK. Carnitine palmitoyltransferase II deficiency: successful anaplerotic diet therapy. Neurology 2008;71:260–264. [PubMed: 18645163]
10. Cox KB, Hamm DA, Millington DS, Matern D, Vockley J, Rinaldo P, Pinkert CA, Rhead WJ, Lindsey JR, Wood PA. Gestational, pathologic and biochemical differences between very long-chain acyl-CoA dehydrogenase deficiency and long-chain acyl-CoA dehydrogenase deficiency in the mouse. Hum. Mol. Genet 2001;10:2069–2077. [PubMed: 11590124]
11. Exil VJ, Roberts RL, Sims H, McLaughlin JE, Malkin RA, Gardner CD, Ni G, Rottman JN, Strauss AW. Very-long-chain acyl-coenzyme a dehydrogenase deficiency in mice. Circ. Res 2003;93:448–455. [PubMed: 12893739]
12. Spiekerkoetter U, Tokunaga C, Wendel U, Mayatepek E, Exil V, Duran M, Wijburg FA, Wanders RJ, Strauss AW. Changes in blood carnitine and acylcarnitine profiles of very long-chain acyl-CoA dehydrogenase-deficient mice subjected to stress. Eur. J. Clin. Invest 2004;34:191–196. [PubMed: 15025677]

13. Exil VJ, Gardner CD, Rottman JN, Sims H, Bartelds B, Khuchua Z, Sindhal R, Ni G, Strauss AW. Abnormal mitochondrial bioenergetics and heart rate dysfunction in mice lacking very-long-chain acyl-CoA dehydrogenase. Am. J. Physiol Heart Circ. Physiol 2006;290:H1289–H1297. [PubMed: 16199475]
14. Kurtz DM, Rinaldo P, Rhead WJ, Tian L, Millington DS, Vockley J, Hamm DA, Brix AE, Lindsey JR, Pinkert CA, O'Brien WE, Wood PA. Targeted disruption of mouse long-chain acyl-CoA dehydrogenase gene reveals crucial roles for fatty acid oxidation. Proc. Natl. Acad. Sci. U. S. A 1998;95:15592–15597. [PubMed: 9861014]
15. Ibdah JA, Paul H, Zhao Y, Binford S, Salleng K, Cline M, Matern D, Bennett MJ, Rinaldo P, Strauss AW. Lack of mitochondrial trifunctional protein in mice causes neonatal hypoglycemia and sudden death. J. Clin. Invest 2001;107:1403–1409. [PubMed: 11390422]
16. Ji S, You Y, Kerner J, Hoppel CL, Schoeb TR, Chick WS, Hamm DA, Sharer JD, Wood PA. Homozygous carnitine palmitoyltransferase 1b (muscle isoform) deficiency is lethal in the mouse. Mol. Genet. Metab 2008;93:314–322. [PubMed: 18023382]
17. Nyman LR, Cox KB, Hoppel CL, Kerner J, Barnoski BL, Hamm DA, Tian L, Schoeb TR, Wood PA. Homozygous carnitine palmitoyltransferase 1a (liver isoform) deficiency is lethal in the mouse. Mol. Genet. Metab 2005;86:179–187. [PubMed: 16169268]
18. He XY, Shoukry K, Chu C, Yang J, Sprecher H, Schulz H. Peroxisomes contain delta 3,5,delta 2,4-dienoyl-CoA isomerase and thus possess all enzymes required for the beta-oxidation of unsaturated fatty acids by a novel reductase-dependent pathway. Biochem. Biophys. Res. Commun 1995;215:15–22. [PubMed: 7575583]
19. Rasmussen JT, Borchers T, Knudsen J. Comparison of the binding affinities of acyl-CoA-binding protein and fatty-acid-binding protein for long-chain acyl-CoA esters. Biochem. J 1990;265:849–855. [PubMed: 2306218]
20. IJlst L, Mandel H, Oostheim W, Ruiter JP, Gutman A, Wanders RJ. Molecular basis of hepatic carnitine palmitoyltransferase I deficiency. J. Clin. Invest 1998;102:527–531. [PubMed: 9691089]
21. van Vlies N, Ruiter JP, Doolaard M, Wanders RJ, Vaz FM. An improved enzyme assay for carnitine palmitoyl transferase I in fibroblasts using tandem mass spectrometry. Mol. Genet. Metab 2007;90:24–29. [PubMed: 16935015]
22. Ventura FV, Costa CG, Struys EA, Ruiter J, Allers P, IJlst L, de Almeida IT, Duran M, Jakobs C, Wanders RJ. Quantitative acylcarnitine profiling in fibroblasts using [U-13C] palmitic acid: an improved tool for the diagnosis of fatty acid oxidation defects. Clin. Chim. Acta 1999;281:1–17. [PubMed: 10217622]
23. Minkler PE, Ingalls ST, Hoppel CL. Strategy for the isolation, derivatization, chromatographic separation, and detection of carnitine and acylcarnitines. Anal. Chem 2005;77:1448–1457. [PubMed: 15732930]
24. Minkler PE, Stoll MS, Ingalls ST, Yang S, Kerner J, Hoppel CL. Quantification of carnitine and acylcarnitines in biological matrices by HPLC electrospray ionization-mass spectrometry. Clin. Chem 2008;54:1451–1462. [PubMed: 18678604]
25. Manning NJ, Olpin SE, Pollitt RJ, Webley J. A comparison of [9,10-3H]palmitic and [9,10-3H] myristic acids for the detection of defects of fatty acid oxidation in intact cultured fibroblasts. J. Inherit. Metab Dis 1990;13:58–68. [PubMed: 2109149]
26. Ramakers C, Ruijter JM, Deprez RH, Moorman AF. Assumption-free analysis of quantitative real-time polymerase chain reaction (PCR) data. Neurosci. Lett 2003;339:62–66. [PubMed: 12618301]
27. Lehman TC, Hale DE, Bhala A, Thorpe C. An acyl-coenzyme A dehydrogenase assay utilizing the ferricenium ion. Anal. Biochem 1990;186:280–284. [PubMed: 2363500]
28. Furuta S, Miyazawa S, Hashimoto T. Purification and properties of rat liver acyl-CoA dehydrogenases and electron transfer flavoprotein. J. Biochem 1981;90:1739–1750. [PubMed: 7334008]
29. Dacremont G, Vincent G. Assay of plasmalogens and polyunsaturated fatty acids (PUFA) in erythrocytes and fibroblasts. J. Inherit. Metab Dis 1995;18:84–89. [PubMed: 9053558]
30. Onkenhout W, Venizelos V, van der Poel PF, van den Heuvel MP, Poorthuis BJ. Identification and quantification of intermediates of unsaturated fatty acid metabolism in plasma of patients with fatty acid oxidation disorders. Clin. Chem 1995;41:1467–1474. [PubMed: 7586519]

31. Aoyama T, Uchida Y, Kelley RI, Marble M, Hofman K, Tonsgard JH, Rhead WJ, Hashimoto T. A novel disease with deficiency of mitochondrial very-long-chain acyl-CoA dehydrogenase. Biochem. Biophys. Res. Commun 1993;191:1369–1372. [PubMed: 8466512]
32. Aoyama T, Souri M, Ushikubo S, Kamijo T, Yamaguchi S, Kelley RI, Rhead WJ, Uetake K, Tanaka K, Hashimoto T. Purification of human very-long-chain acyl-coenzyme A dehydrogenase and characterization of its deficiency in seven patients. J. Clin. Invest 1995;95:2465–2473. [PubMed: 7769092]
33. Wanders RJ, Denis S, Ruiter JP, IJlst L, Dacremont G. 2,6-Dimethylheptanoyl-CoA is a specific substrate for long-chain acyl-CoA dehydrogenase (LCAD): evidence for a major role of LCAD in branched-chain fatty acid oxidation. Biochim. Biophys. Acta 1998;1393:35–40. [PubMed: 9714723]
34. Le W, Abbas AS, Sprecher H, Vockley J, Schulz H. Long-chain acyl-CoA dehydrogenase is a key enzyme in the mitochondrial beta-oxidation of unsaturated fatty acids. Biochim. Biophys. Acta 2000;1485:121–128. [PubMed: 10832093]
35. Yu W, Liang X, Ensenauer RE, Vockley J, Sweetman L, Schulz H. Leaky beta-oxidation of a trans-fatty acid: incomplete beta-oxidation of elaidic acid is due to the accumulation of 5-trans-tetradecenoyl-CoA and its hydrolysis and conversion to 5-trans-tetradecenoylcarnitine in the matrix of rat mitochondria. J. Biol. Chem 2004;279:52160–52167. [PubMed: 15466478]
36. Roe DS, Vianey-Saban C, Sharma S, Zabot MT, Roe CR. Oxidation of unsaturated fatty acids by human fibroblasts with very-long-chain acyl-CoA dehydrogenase deficiency: aspects of substrate specificity and correlation with clinical phenotype. Clin. Chim. Acta 2001;312:55–67. [PubMed: 11580910]
37. He M, Rutledge SL, Kelly DR, Palmer CA, Murdoch G, Majumder N, Nicholls RD, Pei Z, Watkins PA, Vockley J. A new genetic disorder in mitochondrial fatty acid beta-oxidation: ACAD9 deficiency. Am. J. Hum. Genet 2007;81:87–103. [PubMed: 17564966]
38. Kurtz DM, Tolwani RJ, Wood PA. Structural characterization of the mouse long-chain acyl-CoA dehydrogenase gene and 5' regulatory region. Mamm. Genome 1998;9:361–365. [PubMed: 9545492]
39. Zhang Z, Zhou Y, Mendelsohn NJ, Bauer GS, Strauss AW. Regulation of the human long chain acyl-CoA dehydrogenase gene by nuclear hormone receptor transcription factors. Biochim. Biophys. Acta 1997;1350:53–64. [PubMed: 9003458]
40. Ensenauer R, He M, Willard JM, Goetzman ES, Corydon TJ, Vandahl BB, Mohsen AW, Isaya G, Vockley J. Human acyl-CoA dehydrogenase-9 plays a novel role in the mitochondrial beta-oxidation of unsaturated fatty acids. J. Biol. Chem 2005;280:32309–32316. [PubMed: 16020546]

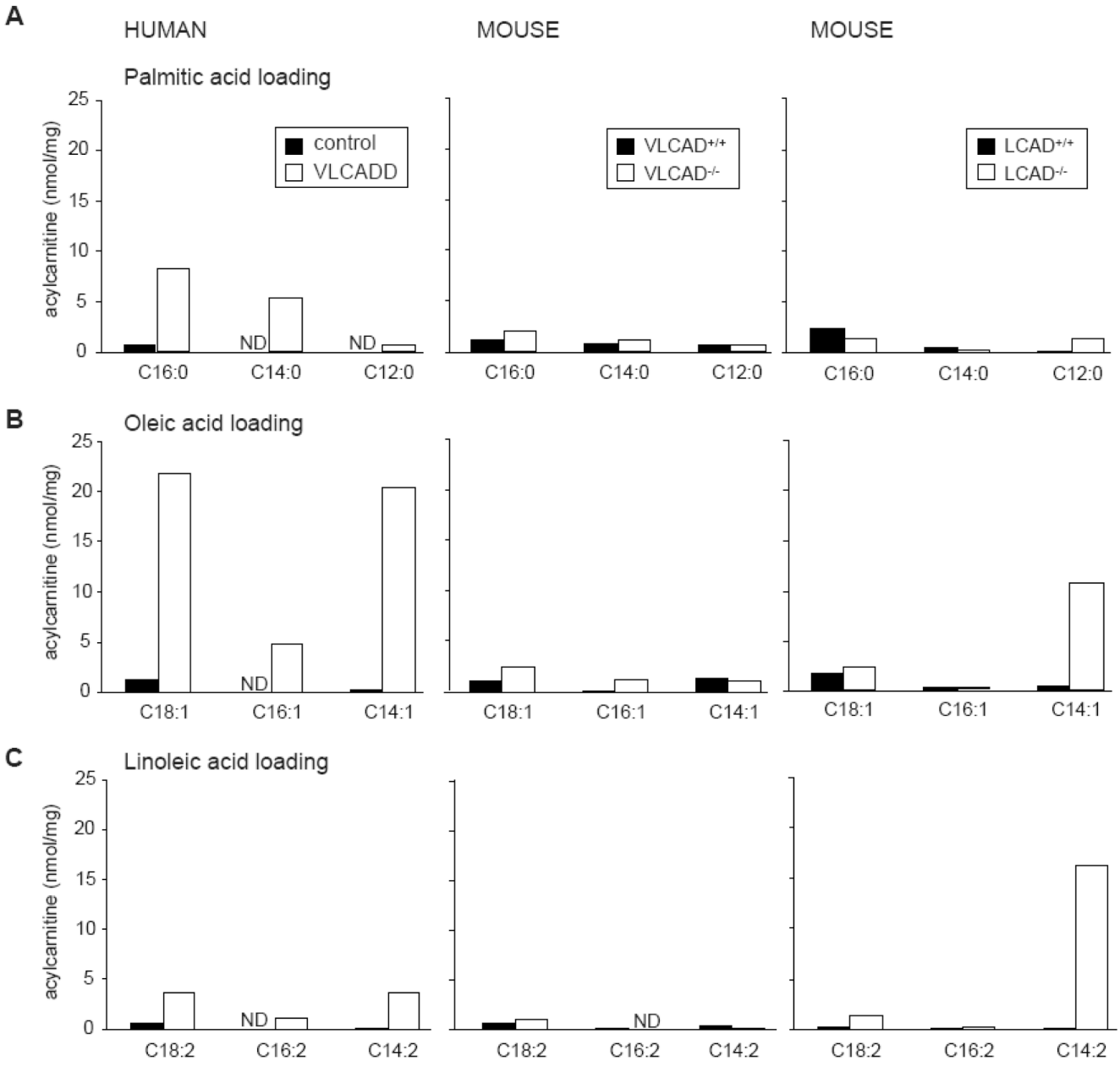

Figure 1.

Acylcarnitine profile analysis by tandem MS. Selected acylcarnitines in medium of human control fibroblasts compared to VLCADD fibroblasts, and wild type mouse fibroblasts compared to VLCAD$^{-/-}$ and LCAD$^{-/-}$ fibroblasts incubated with palmitic acid (A), oleic acid (B), and linoleic acid (C). Data are expressed as nmol/mg protein produced in 72h. Values are the mean concentration of 3 independent incubations. ND denotes not detectable.

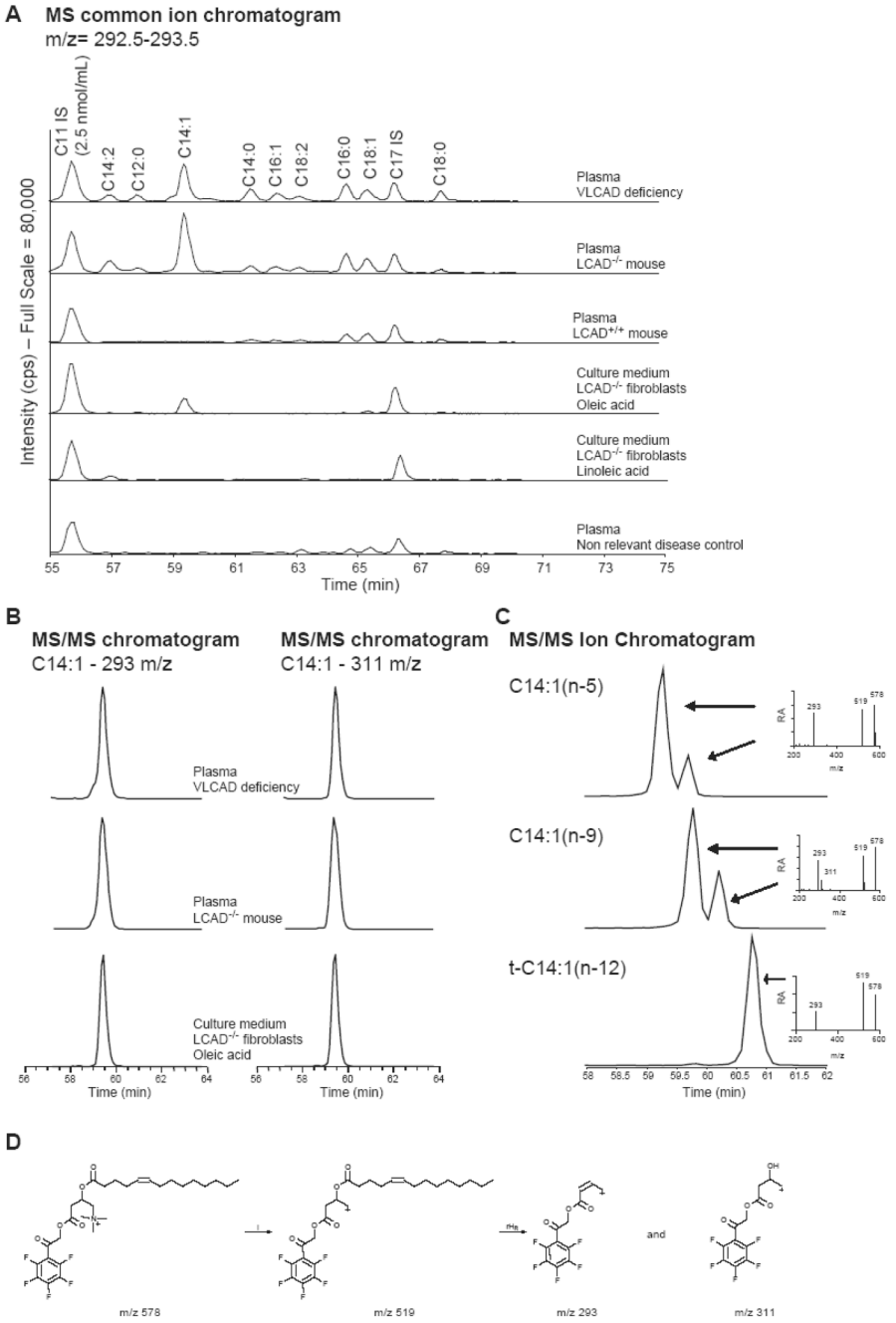

Figure 2.

HPLC MS/MS analysis of acylcarnitine pentafluorophenacyl esters. (A) The full scan MS qualitative chromatogram, with the actual intensity of the common ion (m/z 292.5–293.5) on the y-axis. The concentration of the C11 internal standard (IS) is 2.5 nmol/mL. The figure shows the acylcarnitine profile in plasma of a human VLCADD patient, plasma of a $LCAD^{-/-}$ mouse, plasma of a $LCAD^{+/+}$ mouse, plasma of a human non relevant disease control, medium of $LCAD^{-/-}$ fibroblasts incubated with oleic acid and medium of $LCAD^{-/-}$ fibroblasts incubated with linoleic acid. (B) MS/MS quantitative chromatogram of selected samples for the common (m/z 293) and specific (m/z 311) ion of C14:1 acylcarnitine pentafluorophenacyl ester. (C) Full scan MS/MS chromatogram for C14:1 acylcarnitine and the MS/MS spectrum

for C14:1(n-5), C14:1(n-9), and t-C14:1(n-12) acylcarnitine pentafluorophenacyl ester. (D) Proposed fragmentation of C14:1(n-9) acylcarnitine pentafluorophenacyl ester.

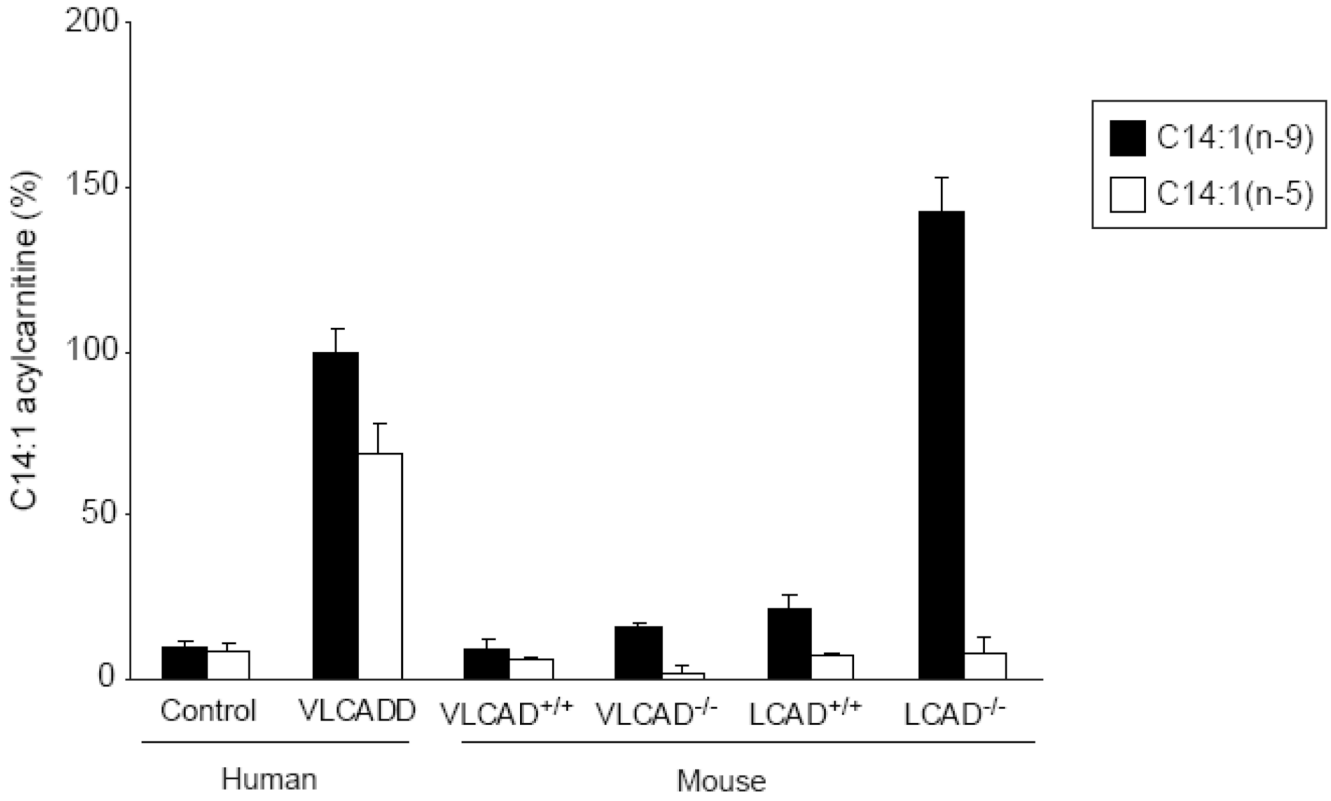

Figure 3.
C14:1 acylcarnitine analysis by tandem MS. Fibroblasts were incubated with 120μM C14:1 (n-9) or 120μM C14:1(n-5). On the y-axis, C14:1 acylcarnitine levels are represented as % with VLCADD fibroblasts loaded with C14:1(n-9) set as 100%.

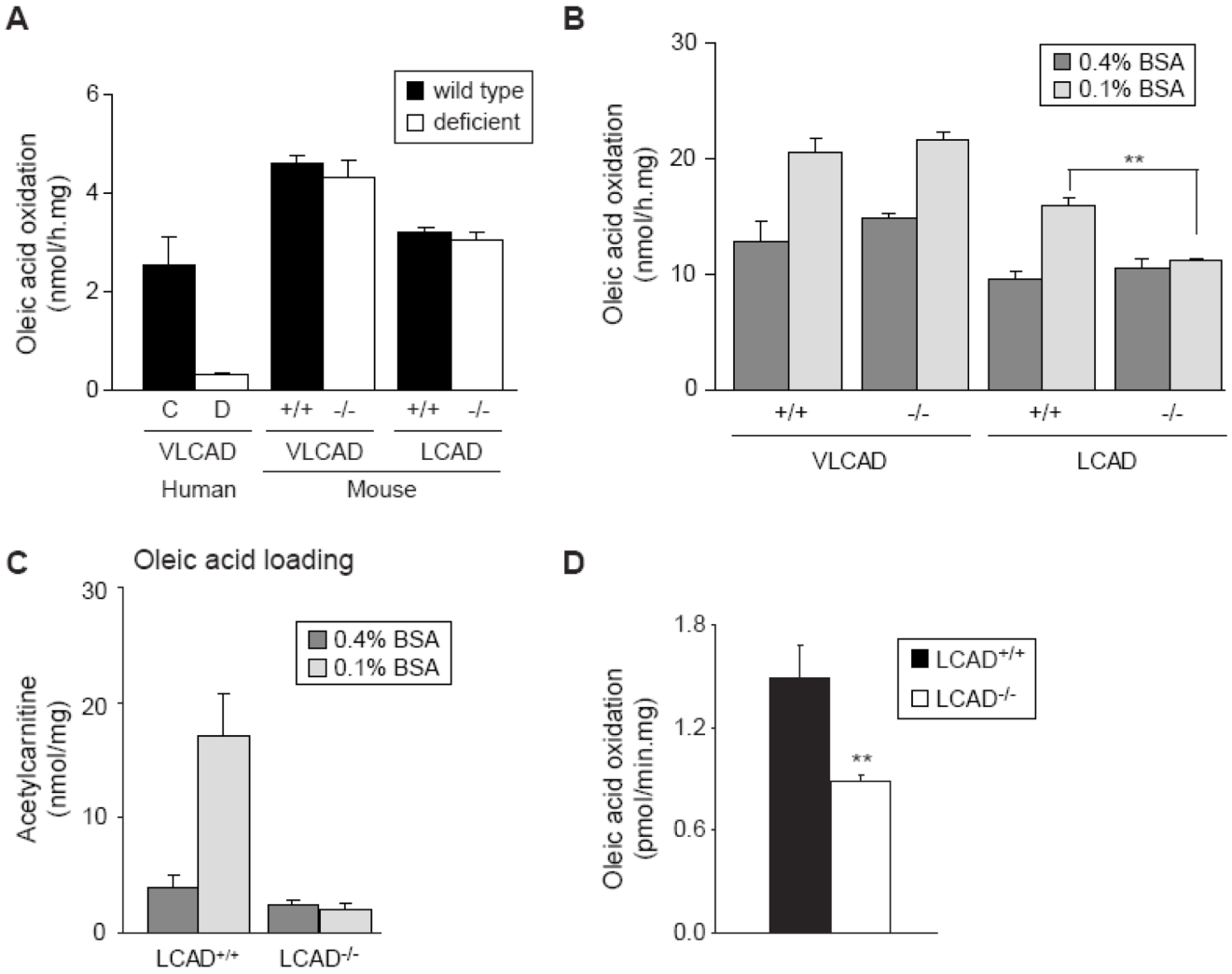

Figure 4.

Differences in oleic acid oxidation between human and mouse fibroblasts. A. Oleic acid oxidation in human VLCADD fibroblasts (D, white bar) compared to control fibroblasts (C, black bar), and VLCAD$^{-/-}$ and LCAD$^{-/-}$ mouse fibroblasts (white bars) compared to wild type fibroblasts (black bars), using 0.4% BSA and 100μM oleic acid. B. Oleic acid oxidation measured with 0.4% BSA and 0.1% BSA in fibroblasts of the VLCAD$^{-/-}$ and CAD$^{-/-}$ mouse compared with wild type fibroblasts. Differences between 0.1% and 0.4% treated cells were analyzed by a paired *t* test, ** denotes P < 0.01. C. C2-acylcarnitine production in fibroblasts of the LCAD$^{-/-}$ and wild type fibroblasts after 72 hr incubation with 100μM [U-^{13}C]-oleic acid, in the presence of 0.4% BSA and 0.1% BSA. D. Oleic acid oxidation in soleus muscle of LCAD$^{+/+}$ and LCAD$^{-/-}$ mice measured using 0.1% BSA and 100mM fatty acid. Differences were analyzed by an unpaired *t* test. ** denotes P < 0.01.

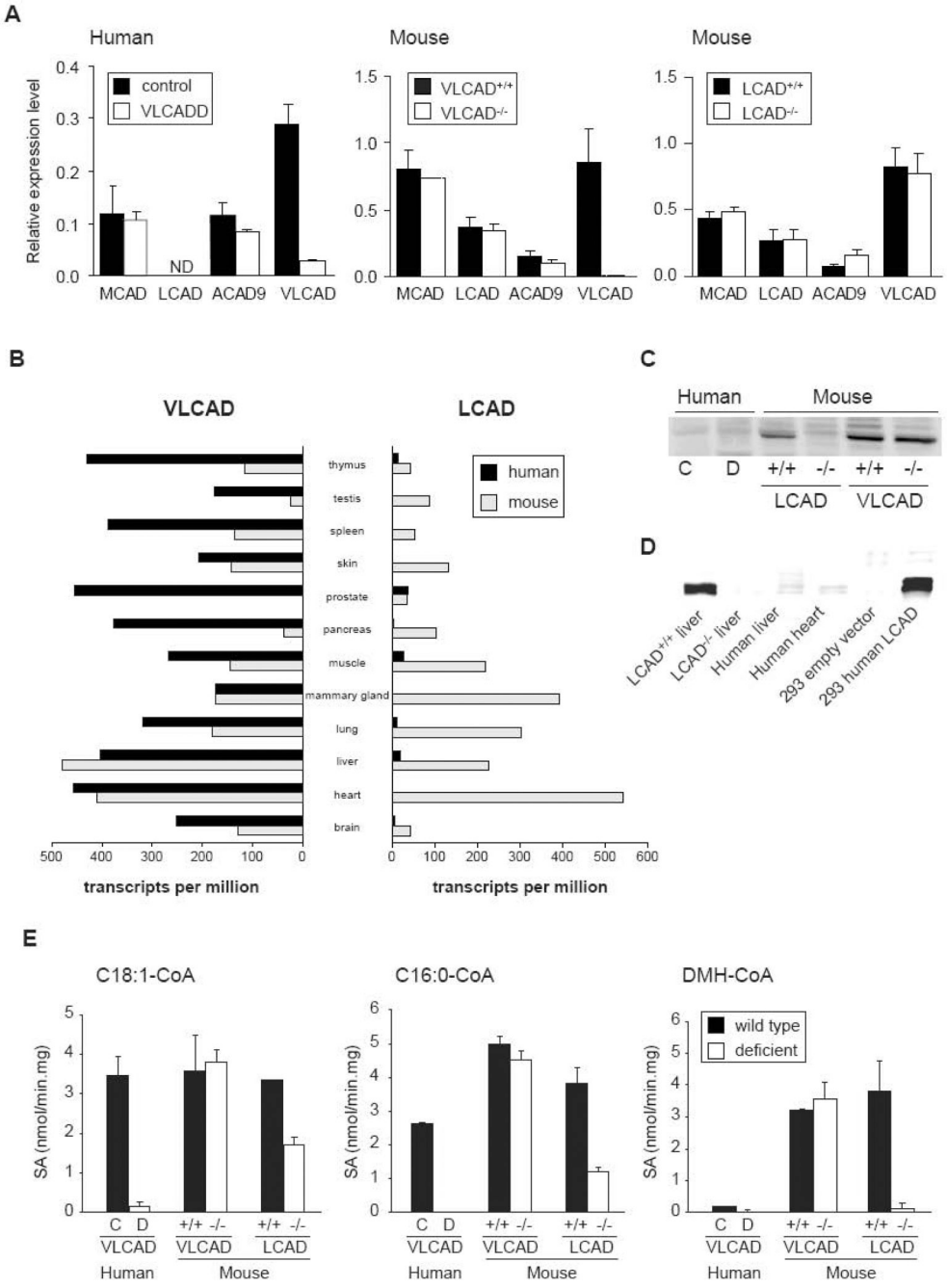

Figure 5.

Expression levels of different acyl-CoA dehydrogenases. A. Gene expression of MCAD, ACAD9, LCAD and VLCAD in human VLCADD fibroblasts compared to control fibroblasts, and fibroblasts of the VLCAD$^{-/-}$ and LCAD$^{-/-}$ mouse compared to wild type fibroblasts, ND denotes not detectable. B. VLCAD and LCAD gene expression in different human and mouse tissue. The gene expression is expressed as the total number of EST per 1 million transcripts. C. Immunoblot analysis of different human and mouse fibroblast extracts (22.5μg of protein per lane) as indicated in the figure using an LCAD antibody. D. Immunoblot analysis of extracts of LCAD$^{+/+}$ and LCAD$^{-/-}$ liver, human liver and human heart (25μg of protein per lane) as indicated in the figure using an LCAD antibody. As a positive control, we overexpressed human

LCAD cDNA in 293 cells. E. Long chain acyl-CoA dehydrogenase activity. Dehydrogenation of C18:1-CoA, C16:0-CoA and DMH-CoA was measured in human control (C, black bars) and VLCADD (D, white bars) fibroblasts, and in mouse wild type (black bars) and $VLCAD^{-/-}$ and $LCAD^{-/-}$ fibroblasts (white bars). SA denotes specific activity.

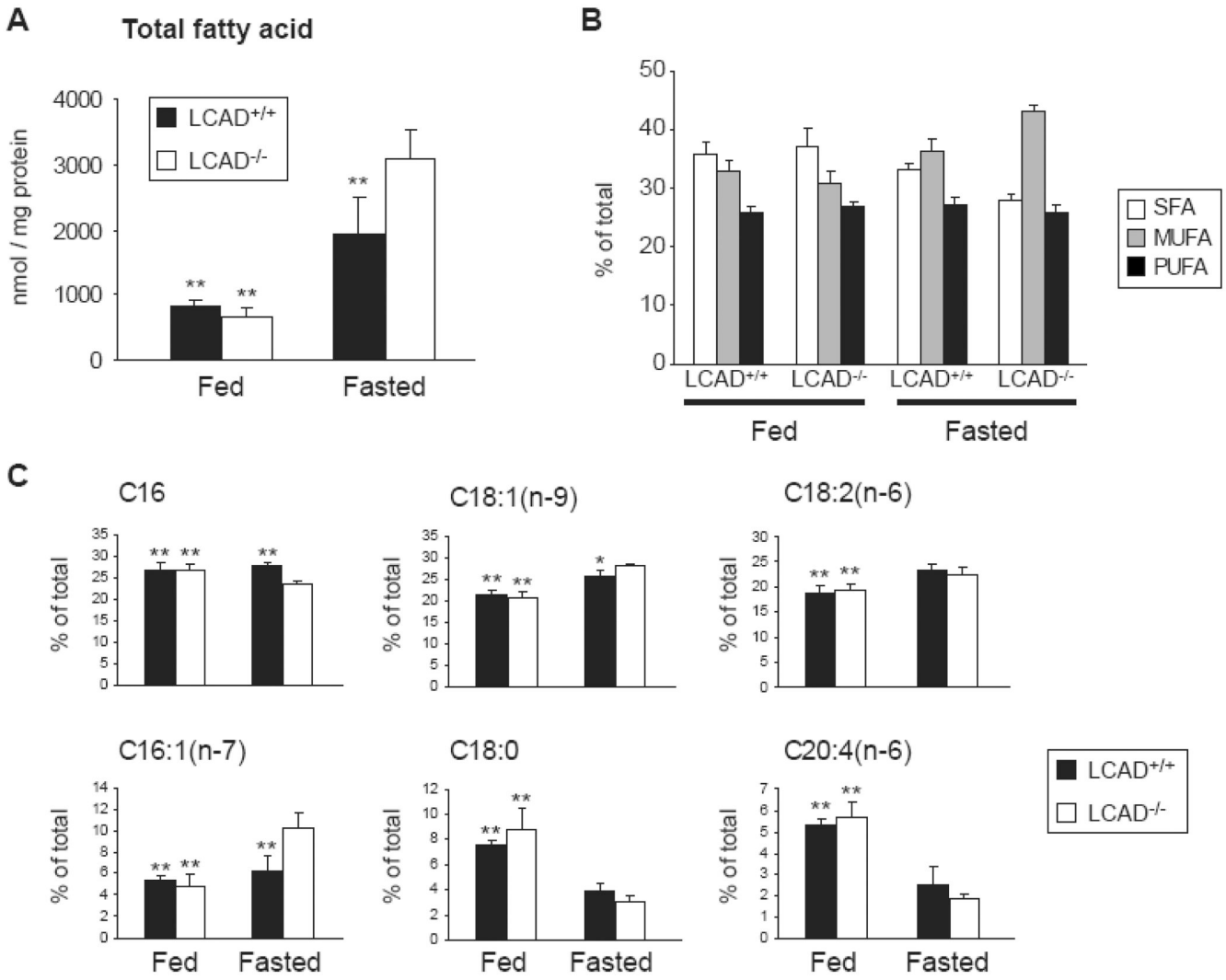

Figure 6.

The fatty acid spectrum in livers of LCAD$^{-/-}$ mice. A. Total hepatic fatty acid content in fed and fasted LCAD$^{+/+}$ and LCAD$^{-/-}$ mice. B. Relative contribution of saturated (SFA), monounsaturated (MUFA) and polyunsaturated fatty acid (PUFA) to the total fatty acids. C. Relative contribution of selected fatty acids to the total fatty acid content. Differences were analyzed by an oneway ANOVA followed by a Dunnett post hoc test. * denotes $P < 0.05$ and **denotes $P < 0.01$.